Identifying and correcting the World War 2 warm anomaly in sea surface temperature measurements

Comments are welcome by contacting the corresponding author directly.

Short title: World War 2 sea surface temperature anomaly

Duo Chan [1]*, Peter Huybers[1]

[1] Department of Earth and Planetary Sciences, Harvard University, USA

*Corresponding author. Email: duochan@g.harvard.edu

Abstract

Most foregoing estimates of historical sea surface temperature (SST) feature warmer global-average SSTs during World War 2 well in excess of climate-model predictions. This warm anomaly, referred to as the WW2WA, was hypothesized to arise from incomplete corrections of biases associated with rapid changes in measurement instruments and protocols. Using linear mixed-effects methods we confirm highly significant offsets among specific groups of bucket and engine-room-intake SST measurements that, upon correction, reduce the WW2WA by 0.26°C (95% c.i. 0.15 to 0.38°C). Furthermore, SST measurements during WW2 coming from buckets are reportedly warmer at night than day, and controlling for this evident bias reduces the WW2WA by another 0.05°C (0.02 to 0.08°C). Adjusted SSTs give a more stable and smoothly evolving record of historical warming with a WW2WA of 0.09°C (-0.01 to 0.18°C) that is consistent with internal variability in climate models.

INTRODUCTION

The two most recent versions of the extended-reconstructed SST (*1, 2*) both show an anomalous warmth in global-mean SSTs that averages 0.28°C during 1941 to 1945 compared with the average over the 10 surrounding years (1936 to 1940 and 1946 to 1950, Fig. 1 and Table 1). Version 4 of the Hadley Center SST (HadSST4) shows a similar anomaly of 0.20°C (*3*). Such a warming anomaly greatly exceeds that produced by any of the 94 historical CMIP5 simulations available over this interval (*4*, gray shading in Fig. 1), as well as what can be explained by current knowledge of climate forcing and internal variability using statistical models (*5*).

If the WW2 Warm Anomaly, WW2WA, reflects physical changes in climate, it would have important implications for understanding the magnitude of decadal climate variability (*6-8*), constraining uncertain external forcing (*9*), and partitioning relative contributions of anthropogenic forcing and internal variability in driving historical climate change (*10-13*). For example, such an anomaly could indicate the ability of the El Niño Southern Oscillation (ENSO) to lead to larger and more persistent warming than is typically observed (*14*).

However, the physicality of the WW2WA is questionable. Different instrumental estimates disagree on the SST evolution during WW2 (Fig. 1). Despite highly significant warm spikes in ERSSTs and HadSST4, HadSST2 (*15*) was shown to exhibit a step in global-average SST of 0.3°C once the effects of variations in Niño and ocean-land atmospheric effects were filtered from the global average (*16*), and the WW2WA was essentially absent in HadSST3 (*17*). Furthermore, neither air temperatures from near-shore weather stations (*18*) nor temperature proxies derived from isotopes in Tropical coral reefs (*19*) show a similar WW2 anomaly.

Hypothesized causes and existing corrections

The presence of discontinuities in the SST record appears especially likely an artifact because of a major transition in instruments (*16*) changes in protocols (*20*), and a 58% reduction in the number of SST measurements during the WW2 interval (*17*). It has been suggested that the WW2WA occurs because the dominant data-collecting instrument alternates from buckets in the five years prior and post WW2 to engine-room-intake (ERI) during 1941 to 1945 (*16*). Bucket SSTs are generally biased cold from evaporative and sensible cooling, with the cold bias of a typical U.K. canvas bucket estimated to average 0.4°C (*21*). Conversely, although ERI measurements are typically extracted from 5 to 15m below the surface and are consequently cooler than true SSTs defined at depths of 20 to 30 cm (*3*). ERI SSTs have an average warm bias of 0.1 to 0.3°C because of absorption of heat from ship engines (*3, 17*).

A second hypothesis involves changes in protocols for taking measurements at night. Night-time marine air temperature reading is known to have been taken in-board in order to avoid detection and, consequently, to be warmly biased by approximately 0.8°C (*20*). We speculate that bucket SSTs were also read in-board during WW2. The fact that the proportion of SST readings during day shifts from 55% of the total in the surrounding ten years of the war to 61% between 1941 and 1945 also suggests a preference for avoiding night-time readings. Incomplete corrections of biases among ERI and bucket measurements could be responsible for the WW2WA.

The six major SST estimates covering the WW2 period each account for SST biases using distinct methods. Because these estimates all rely upon data coming from the International Comprehensive Ocean-Atmosphere Data Set (ICOADS, *22*), differences among estimates generally arise from differences in correction schemes that can be divided into two groups. In one

63   approach, bucket and ERI measurements are not distinguished and average SSTs are corrected to

64   follow independent estimates of temperatures. For example, ERSST5 (*2*) is referred to Hadley

65   night-time marine air temperatures (*23*), from which the global average inherits a 0.22°C warm

66   anomaly during WW2 relative to the ten surrounding years. Note that our taking the average

67   between 1941 and 1945 relative to the average over the prior and subsequent five years accounts

68   for the potential of an underlying linear trend between 1936 and 1950. Ship-based air temperatures

69   are, however, potentially subject to their own biases on account of non-standard measurement

70   practices (*20*) and reconstruction choices (*23*) during WW2. Another example is to reference SSTs

71   to air temperature from coastal and island weather stations, in which case the WW2 SST anomaly

72   is removed (*18*).

73   A second approach to correcting SSTs distinguishes between bucket and ERI

74   measurements and attempts to correct their respective biases (*3, 17*). A major impediment to such

75   corrections, however, is that measurement methods are poorly documented during WW2, with

76   only 6% of observations being specifically documented as coming from buckets, 11% from ERIs,

77   and 83% undetermined (*22, 24*). The magnitudes of SST biases are also uncertain, and, as noted,

78   may have changed during WW2 (*20, 23*). The lack of information regarding measurements has

79   been addressed through plausible but uncertain assumptions. In constructing HadSST3, for

80   example, it was assumed that U.S. and U.K. naval ships with unknown methods make ERI

81   measurements of SST that are, on average, warmly biased by 0.2°C (*17*). HadSST4, however,

82   randomly designates unknown measurements during WW2 to be either bucket or ERI SSTs, with

83   the portion of bucket measurements ranging from 0 to 25%. Wartime ERI measurements in

84   HadSST4 are specified to have a 0.25°C warm bias, on average, whereas buckets are specified to

85   have a -0.2°C cold bias (*3*).

86   **RESULTS**

87   **Groupwise SST offsets**

88   We examine hypotheses that changes in instrumental and measurement protocols account for the

89   WW2WA using a linear-mixed-effects (LME) methodology.   This LME method was recently

90   shown to accurately identify offsets among groups of bucket SST measurements in the ICOADS

91   dataset (*25,26*), and we extend the approach to encompass ERI measurements (Fig. S1).   SST

92   measurements coming from distinct groups that are within 300 km and 2 days of one another are

93   differenced (Fig. 2D), and systematic structures in the differences are partitioned among regional,

94   seasonal, temporal, and groupwise offsets.   Groups are defined according to instrument type,

95   nation, and 'decks', where the term 'deck' originally refers to punch cards that marine observations

96   were encoded upon (*22*). Although decks were not necessarily originally organized according to

97   physical features, in practice, there are major offsets between different decks of bucket

98   measurements (*25*).   Variance not attributable to systematic offsets by our LME method is

99   considered noise that is parameterized in relation to location, season, and distance in space and

100 time between measurements (see methods).   Importantly, the LME methodology permits for

101 obtaining groupwise offsets regardless of whether the method of measurement is known.

102   Of the 66 groups present between 1935 and 1949, 29 have significant offsets ($P<0.05$,

103 Table S1). Significance is assessed relative to a null hypothesis of zero-mean offset with respect

104 to the average across all groups.   After correcting for multiple hypothesis testing using a

105 Bonferroni correction, 12 groups still show significant offsets ($P<0.05/n$, n=66). There are five

106 positively identified ERI groups that are found to be warmer than the 24 bucket groups, on average,

107 by 0.53°C (0.25 to 0.72°C, Table S1). All uncertainties are reported as 95% coverage intervals

108 unless otherwise noted. Offsets of unknown groups range from -0.4 to 0.6°C, a range similar to

109   that spanned by the entire population of the bucket and ERI groups, suggesting that at least some

110   of these groups are distinctly from bucket or ERI measurements.

111   A check of our estimated groupwise offsets is afforded through comparing against the

112   amplitude of the diurnal cycle associated with individual groups. ERI measurements typically

113   come from greater depths and, thus, exhibit a smaller amplitude diurnal cycle than actual SSTs,

114   whereas buckets are subject to solar gain and generally exhibit a larger amplitude diurnal cycle

115   (*27*). A strong correlation emerges between diurnal amplitudes and offsets among groups

116   consistent with many groups containing a mixture of bucket and ERI measurements (*28*).

117   Extending the same techniques to measurements of unknown origin (Fig. 3), we find that most

118   U.S. measurements that are biased warm also exhibit a small diurnal amplitude, consistent with

119   their being ERI measurements. Specifically, five U.S. groups (deck 110, 116, 195, 281, and 705)

120   account for 88% of all U.S. measurements during 1935 to 1949 and each is significantly warmer

121   than the average across all groups ($P<0.05$, Fig. 3, Table S1) and exhibits a diurnal amplitude that

122   is significantly smaller ($P<0.05$, Fig. 3, Table S1, and Fig. S2) than a climatology derived from

123   drifting buoys (see methods). The combination of warm offsets and small diurnal amplitudes

124   confirm the assumption in HadSST3 that U.S. measurements with missing method information

125   during WW2 are ERI measurements.

126   Although it is not necessary to identify the instrumental origin of measurements in order

127   for our method to estimate and correct for offsets, we first make a provisional classification of

128   measurements with unknown instrumental information for purposes of estimating SSTs using

129   bucket-only and ERI-only measurements. In particular, we assign all U.S. ships of unknown origin

130   to ERIs because of their anomalously warm offsets and anomalously small diurnal amplitudes

131   (Table S1). Estimates of global-average SSTs using only observations thought to come from ERIs,

132   0.09°C, or buckets, 0.19°C, are stable through WW2 relative to the warming shown in the raw

133   ICOADS data, 0.41°C (Fig. 2A), confirming that the anomaly mainly reflects instrumental changes

134   at the start and the end of the war (*16*).

135   Our main line of reconstruction of historical SSTs during WW2 relies on combining all

136   groups of SSTs together after correcting for groupwise offsets, which gives an estimate of global

137   SSTs featuring a WW2WA that is decreased from 0.41°C in the raw ICOADS measurements (Fig.

138   2A) to 0.14°C (0.02 to 0.27°C) in the groupwise corrected SSTs (Fig. 2B). Groupwise adjusted

139   SSTs are consistent between bucket and ERI-only estimates, with collocated ERI minus bucket

140   difference decreasing from an average of 0.48°C over 1936 to 1950 in raw ICOADS3.0 to being

141   centered on zero after adjustments (Fig. 2C).

142   Diminishment of the WW2WA reflects negative adjustments of SSTs from U.S. Navy ship

143   logs (deck 195) that have a warm offset of 0.43°C (0.17 to 0.68°C) that alone brings the WW2WA

144   from 0.41°C in raw ICOADS to 0.22°C (Fig. 2E). Also of note are U.K. Royal Navy ship logs

145   (deck 245) that have a data gap in 1940 (Fig. S1A) and offsets that are -0.31°C (-0.53 to -0.09°C)

146   cold before 1940 and 0.25°C (0.03 to 0.47°C) warm over 1941-1947 (Fig. 3). Adjusting offsets in

147   deck 245 contributes another 0.06°C to the diminishment of the WW2WA (Fig. 2E), with the

148   largest local decrease of more than 0.4°C over the Indian Ocean and the Pacific Warm Pool.

149   **Night-time bucket SSTs**

150   The second hypothesis we test is whether warm biases arise as a result of measuring bucket SSTs

151   in-board during the night. When isolated, raw night-time bucket measurements contain a 0.32°C

152   warm anomaly during the war (Fig. 4A). Night-time SSTs reverse from being cooler than

153   collocated daytime temperatures by -0.20°C during the five years before and after WW2, as

154   expected regardless of bucket design (28) to actually being 0.02°C warmer during WW2.

155   Spatially, warm WW2 night-time bucket SSTs are found over the Indian Ocean and the extra-

156   tropical Atlantic (Fig. 4B). No such night-time-warming anomaly is found in measurements

157   coming from ERIs. Furthermore, the WW2WA is consistent between raw daytime bucket SSTs

158   (0.10°C, Fig. 4A) and raw daily-mean ERIs (0.09°C, Fig. 2A and 4C).

159   The inversion of the diurnal cycle in bucket SSTs during WW2 is mainly attributable to

160   British Navy ships (deck 204) that contribute more than 75% of open-ocean bucket SSTs during

161   1942 to 1945. (SST observations from buckets that are concentrated near shore have little overall

162   influence on global SST estimates after gridding.) When resolved at the hourly resolution, SST

163   anomalies from deck 204 show a diurnal cycle that peaks at 4 pm and has a diurnal amplitude that

164   is 0.04°C higher than drifters in the ten years surrounding WW2. During WW2 the diurnal peak

165   of deck 204 occurs at 8 pm, and the amplitude of the diurnal cycle is 0.03°C smaller than drifters

166   (Fig. S3). The smaller diurnal amplitude is unlikely to relate to switching to ERI measurements

167   in decks 204 because the average temperature of daytime measurements remains both consistent

168   with bucket measurements and cooler than known ERI measurements taken before and after WW2.

169   These results are consistent with both night-time marine air temperatures (*20*) and bucket

170   temperatures being measured in-board during WW2. British Naval group deck 245 exhibits a

171   similar, albeit less dramatic, decrease in the amplitude of the diurnal cycles (Fig. 3).

172   Although our LME method could be further extended to temporally resolve anomalies in

173   night-time biases, building in such flexibility would essentially make night-time temperatures

174   uninformative. Instead, we simply repeat our analysis using only daytime measurements.

175   Specifically, we use 24.1 million pairings of SST measurements between 1850 and 2014 with 1.1

176   million of these pairs available between 1935 and 1950. Whereas using both day and night

177 measurements gives a 0.14°C (0.02 to 0.27°C) WW2WA, the daytime-only analysis gives a

178 WW2WA of 0.09°C (-0.01 to 0.18°C, Table 1, Fig. S4). Sampling hourly-resolved climatological

179 diurnal cycles from drifters indicates that the shift from 55% of observations occurring in the

180 daytime in the five years before and after WW2 to 61% during WW2 accounts for only 0.005°C

181 of the anomaly, with the systematically warmer night-time temperatures inferred to account for

182 the majority of the difference.

183   The CMIP5 ensemble of 25,236 years of pre-industrial simulations indicates a 0.10°C

184 anomaly in global SSTs as the 95% value for all 15-year intervals (see methods). The residual

185 warm anomaly found after groupwise correction to daytime-only data, therefore, accords with

186 internal SST variability (Fig. 5B). Also consistent with internal variability are bucket-only

187 estimates of SST, having a WW2WA of 0.08°C (-0.02 to 0.17°C) and ERI-only estimates having

188 an anomaly of 0.04°C (-0.07 to 0.14°C). This revision from SST anomalies being highly

189 inconsistent between observations and simulations during WW2 to being consistent, after

190 accounting for observational biases, may also point to a means of resolving the greater SST

191 variance in observational data relative to simulations found at decadal and longer timescales (*29*).

192 **DISCUSSION**

193 **Comparison with other estimates**

194 The SST adjustments obtained through our LME approach agree with an independent estimate

195 arrived at using near-shore, land-station data (*18,* Fig. 5A). Whereas the approach of ref. (*18*)

196 requires average SSTs to agree with land-station data, our analysis shows that the WW2 warm

197 anomaly is an artifact arising from specific groups and features of SST measurements. Our results

198   confirm the assumption made in ref. (*18*) that trends derived from land-station data are more

199   dependable during WW2 than those coming from uncorrected SSTs.

200   Compared with corrections in HadSST, our groupwise intercomparison suggests that ERI

201   and bucket groups have an average offset of 0.53°C (0.25 to 0.72°C), nearly 0.1°C greater than the

202   0.45°C difference used in HadSST4. Furthermore, our analysis indicates that unknown U.S. and

203   U.K. measurements during 1942 to1945, which account for 98% of unknown wartime

204   measurements, are offset warm. In HadSST4, 12.5% of the unknown measurements were assumed

205   to be offset cold and corrected as if from buckets. The smaller offset assumed between bucket and

206   ERI SSTs and a higher percentage of observations assumed to come from buckets explains the re-

207   emergence of the WW2WA in HadSST4. Finally, whereas HadSST4 assumes large uncertainties

208   in data origin during WW2, our analysis uses relative offsets to provide corrections and reduces

209   the standard error of WW2WA from 0.14°C in HadSST4 to 0.05°C in our estimates.

210   An important attribute of groupwise adjustments is the ability to resolve regional biases

211   arising from spatially heterogeneous distributions of distinct groups (Fig. S5). Removing

212   groupwise offsets leads to a greater decrease in the WW2WA over the Indian ocean and Pacific

213   Warm Pool and smaller decreases over the Tropical Eastern Pacific and the South Atlantic (Fig.

214   S5B). The spatial correlation of WW2 anomalies between our adjustments and adjusted daytime-

215   only estimates is $r_s = 0.02$, where r_s indicates the Pearson corss-correlation taken across space and

216   its small value indicates that the magnitude of the pattern that we remove is appropriate. HadSSTs

217   partially accounts for biases associated with shifting instruments and has a similar pattern of

218   correction albeit one that is smaller such that $r_s = -0.15$ (Fig. S5E) for HadSST3 and -0.18 for

219   HadSST4 (Fig. S5F). In contrast, ERSST products use a fixed spatial pattern (*1,2*) that is unable

220   to correct for local patterns of spatial bias giving a $r_s = -0.30$ for ERSST4 (Fig. S5D) and $r_s = -$

221   0.31 for ERSST5. The zonally symmetric corrections from ref. (*18*) are also ineffective at

222   removing the WW2 pattern of offsets.

223   In addition to the removal of the WW2WA, our adjustments give a more stable and smoothly

224   evolving SST estimate (table 1). The 1936 to 1950 variance of global-average, annual SST

225   anomalies decreases from $5.6 \times 10^{-2} °C^2$ in ICOADS raw to $0.5 \times 10^{-2} °C^2$ in the adjusted daytime-

226   only estimates. Such sub-decadal variability is consistent with estimates from HadSST3 and

227   Cowtan SST and lies within the 95% confidence interval of CMIP5 simulations. In contrast,

228   HadSST4 and ERSSTs have significantly higher variance estimates (*P*<0.05). On regional scales,

229   the effect of groupwise adjustments is smaller compared with physical variability, sampling

230   uncertainty, and random measurement errors, such that the 1936 to1950 variance on $5°\times5°$ grids

231   decreases by approximately 20%, on average.

232   **Conclusion**

233   The WW2WA in instrumental SST estimates has long been suggested to be a data artifact that

234   arises from instrumental changes (16). Our analysis confirms the existing hypothesis, identifies

235   warm biases in WW2 night-time SSTs, and provides corrections that remove the WW2WA at both

236   global and regional scales. This adjustment leads to a more homogeneous trend in SSTs and

237   reconciles the largest discrepancy between historical surface temperatures and models (5),

238   bringing SST estimates into accord with estimates of forcing, climate sensitivity, and internal

239   variability. Our results also highlight the importance of further resolving heterogeneity in

240   historical SSTs (24, 26, 30, 31). Adjusting measurements at the level of individual ships (32, 33)

241   in future work may permit more detailed corrections and may reveal even more homogeneous

242   trends in SST.

243   **Materials and Methods**

244   **Grouping**

245   After the same quality control procedures as in ref. (*25*), sea surface temperatures (SSTs) from

246   ICOADS 3.0 (*22*) are grouped according to nation, deck, and measurement method.   Nation is

247   identified first using ICOADS country code (C1, *22*). When C1 is not available, nation is inferred

248   from ship call signs (*26, 28*) or deck information (*17, 25*). If still unidentified, nations information

249   is considered missing, and associated SSTs are grouped only according to deck and method

250   information. Deck is the primary metadata for tracking ICOADS data collections and is available

251   for all SST measurements in ICOADS. Decks having the same description in ICOADS and are

252   combined as in ref. (*28*). Measurement method is identified from ICOADS SST measurement

253   method (SI) metadata. When SI is not available, we use information from the World Meteorology

254   Organization No. 47 publication (WMO No.47). If both are not available, we assign measurement

255   method to be unknown. There are cases that SI and WMO No.47 do not agree (*27*), this, however,

256   does not affect results during WW2 because WMO No.47 becomes available in ICOADS after the

257   1960s.

258   **Groupwise adjustment**

259   Groupwise adjustments to SSTs are estimated using a linear-mixed-effects (LME) model,

260    $\delta\mathbf{T} = \mathbf{X\alpha} + \mathbf{Z}_y\boldsymbol{\beta}_y + \mathbf{Z}_r\boldsymbol{\beta}_r + \boldsymbol{\beta}_\sigma$ (1)

261   The vector of temperature differences, $\delta\mathbf{T}$, is determined from pairs of SST observations that are

262   associated with different nation-deck-method group assignments and are within 300 km and 2 days

263   of one another. All SST measurements that are identified to come from bucket, ERI, hull sensor,

264   or unknown methods between 1850 and 2014 are analyzed for purposes of fully accounting for

265   information outside WW2 of focus. We identify a total of 45.8 million pairs of SSTs, which

266   comprises a subset of 1.8 million SST differences during 1935 to 1950.

267   SST differences contained in $\delta\mathbf{T}$ are represented as a `fixed-effect' term describing offsets

268   between groups, $\boldsymbol{\alpha}$, and random effects describing temporal variations (five-year blocks), $\boldsymbol{\beta}_y$, and

269   regional variations (17 sub-basin regions), $\boldsymbol{\beta}_r$. Matrices $\mathbf{X}$, $\mathbf{Z}_y$, and $\mathbf{Z}_r$ specify, respectively,

270   common pairs of nations, five-year blocks, and sub-basins. $\boldsymbol{\beta}_\sigma$ is the residual. Offsets are estimated

271   relative to the mean of all paired measurements.

272   More details on the LME design and implementation is available in a methodology paper

273   (*25*). In an update to ref. (*25*), the analysis presented here intercompares both bucket and engine-

274   room-intake SSTs and, therefore, yields a total of 492 groups each contributing to at least 5,000

275   pairs of SST observations. In addition, to account for seasonal variations in groupwise offsets,

276   LME models are run for subsets of consecutive three months and repeated twelve times with the

277   central month sliding from January to December. Months of Southern Hemisphere SSTs are

278   shifted by half of a year to account for different seasons between hemispheres.

279   Uncertainties of groupwise offsets, ϵ_g, are quantified by the LME methodology and

280   associated 95% c.i. of individual offsets are estimated as marginal distributions assuming that

281   offsets follow a multivariate normal distribution (*25*). As noted in previous studies (*26, 34*),

282   random errors (ϵ_r) that arise from partial sampling and observational noise become negligible under

283   global and decadal averaging, whereas ϵ_g is partially systematic. We, therefore, only quantify and

284   report uncertainties that stem from ϵ_g for adjusted SSTs. Uncertainties in groupwise adjustments

285   are realized by a 1000-member ensemble of random adjustments that perturb groupwise offsets

286   using their error estimates in keeping with covariance and spatial structures (*26*).

287   The LME method estimates groupwise offsets relative to the mean of all paired

288   measurements and does not account for common biases shared by all groups. Biases between

289   bucket and engine-room-intake measurements may vary with time. One example is that night-

290   time SSTs are abnormally warm from 1941 to 1945 (Fig. 4A), which increases common biases

291   during WW2 and results in a residual warm anomaly after adjusting for groupwise offsets. To

292   exclude the influence of WW2 biases in night-time SSTs, we perform another LME analysis with

293   the same model setup but using only daytime measurements. The daytime-only analysis makes

294   use of a total of 24.1 million SST pairs throughout 1850 to 2014, with a subset of 1.1 million pairs

295   between 1935 and 1950. Another example of changing common biases involves systematic

296   changes from less-insulated canvas to more-insulated rubber buckets (*17*). However, the overall

297   change in bucket types have been estimated to happen after the 1950s (*17*) or gradually take place

298   from the 1930s to the 1970s (*3*). In either case, the associated changes in common biases will have

299   a small influence on the WW2WA.

Diurnal Cycle

301   Recent studies (*27, 28*) illustrate the utility of using the diurnal cycle for better understanding

302   biases in historical SST measurements. In this study, diurnal cycles of individual groups are

303   calculated using tracked ships (*35*) following the methodology of ref. (*28*). Only 33 out of 66 ship

304   groups have acceptable estimates of diurnal cycles, whereas the others have issues arising from

305   lack of tracked ships or insufficient measurements distributed across the day. Diurnal amplitudes

306   are estimated using data between 1935 and 1949 using a leas-squares fit of a once-per-day sinusoid

307 (*28*). The diurnal amplitude of U.S. deck 195 is determined by a least-squares fit using the diurnal

308 cycles determined from bucket- and ERI-only measurement, where this special approach is taken

309 because of the large number of measurements U.S. deck 195 contributes buts its having an

310 insufficient sampling frequency to independently constrain its amplitude (see Fig. S2 for more

311 details). To account for distinct spatial and seasonal coverage of individual groups, reported

312 diurnal amplitudes in Fig. 3 are anomalies relative to 1990 to 2014 climatological amplitudes

313 estimated from drifting buoys (*25*). The scaling between diurnal amplitudes and groupwise offsets

314 is estimated using a York regression (*36*) and associated uncertainties are estimated by

315 bootstrapping individual groups 10,000 times with replacement.

Comparison with other estimates

317 There are different versions of the ICOADS dataset that have been used in various studies, but

318 these differences should have limited influence on SST biases during WW2. First, whereas

319 Cowtan SST (*18*), HadSST3 (*17*), and ERSST4 (*1*) are based on ICOADS2.5 (*37*), our adjusted

320 SSTs, HadSST4 (*3*), and ERSST5 (*2*) are based on ICOADS3.0 (*22*). Compared with 7.4 million

321 measurements over 1935 to 1949 in ICOADS2.5, ICOADS3.0 only includes an additional 17

322 thousand measurements from the U.S. lightship collection. Second, we make use of only ship-

323 based measurements, but other datasets also make use of measurements from moored and drifting

324 buoys and the coastal-marine automated network, but which only become available after the 1980s.

325 Third, ERSSTs and Cowtan SST infill monthly grid boxes without data, but our estimates and

326 HadSSTs leave these boxes unfilled.   Finally, ERSSTs and Cowtan SSTs provides only central

327 estimates, whereas our adjusted SSTs and HadSSTs provide publicly available ensembles that

328 allow for estimating uncertainties associated with corrections.

329   To compare in-situ SST estimates with model simulations, we make use of 94 historical

330 runs from 39 CMIP5 models and a total of 25,236 years of pre-industrial simulations (*4*) that we

331 re-grid to a common 5° resolution. Pre-industrial runs are segmented into consecutive 15-year

332 segments. We then mask each historical run using the monthly coverage in ICOADS3.0 and each

333 15-year pre-industrial segment using the ICOADS coverage between 1936 and 1950. The mean

334 difference between the central five years (1941 to 1945) and surrounding ten years (1936 to 1940

335 and 1946 to 1950) is then calculated for individual pre-industrial segments (historical runs).

336

337 **References**

338 1. Huang, B. et al. Extended reconstructed sea surface temperature version 4 (ERSST. v4).

339   Part I: Upgrades and intercomparisons. Journal of Climate 28, 911–930 (2015).

340 2. Huang, B. et al. Extended reconstructed sea surface temperature, version 5 (ERSSTv5):

341   upgrades, validations, and intercomparisons. Journal of Climate 30, 8179–8205 (2017).

342 3. Kennedy, J., Rayner, N., Atkinson, C. & Killick, R. An ensemble data set of sea surface

343   temperature change from 1850: The Met Office Hadley Centre HadSST. 4.0.0.0 data set.

344   Journal of Geophysical Research: Atmospheres 124, 7719–7763 (2019).

345 4. Taylor, K. E., Stouffer, R. J. & Meehl, G. A. An overview of CMIP5 and the experiment

346   design. Bulletin of the American Meteorological Society 93, 485–498 (2012).

347 5. Folland, C. K., Boucher, O., Colman, A. & Parker, D. E. Causes of irregularities in trends

348   of global mean surface temperature since the late 19th century. Science Advances 4,

349   EAAO5297 (2018).

350 6. Hansen, J., Ruedy, R., Sato, M. & Lo, K. Global surface temperature change. Reviews of

351   Geophysics 48 (2010).

352 7. Morice, C. P., Kennedy, J. J., Rayner, N. A. & Jones, P. D. Quantifying uncertainties in

353   global and regional temperature change using an ensemble of observational estimates: The

354   HadCRUT4 data set. Journal of Geophysical Research: Atmospheres 117 (2012).

355 8. Vose, R. S. et al. NOAA's merged land–ocean surface temperature analysis. Bulletin of

356   the American Meteorological Society 93, 1677–1685 (2012).

357 9. Stevens, B. Rethinking the lower bound on aerosol radiative forcing. Journal of Climate

358   28, 4794–4819 (2015).

359 10. Jones, G. S., Stott, P. A. & Christidis, N. Attribution of observed historical near–surface

360   temperature variations to anthropogenic and natural causes using CMIP5 simulations. Jour-

361   nal of Geophysical Research: Atmospheres 118, 4001–4024 (2013).

362 11. Bindoff, N. L. et al. Detection and attribution of climate change: from global to regional

363   (2013).

364 12. Maher, N., Gupta, A. S. & England, M. H. Drivers of decadal hiatus periods in the 20th

365   and 21st centuries. Geophysical Research Letters 41, 5978–5986 (2014).

366   13. Hegerl, G. C., Bro̎nnimann, S., Schurer, A. & Cowan, T. The early 20th century warming:

367   anomalies, causes, and consequences. Wiley Interdisciplinary Reviews: Climate Change 9,

368   e522 (2018).

369   14. Thompson, D. W., Wallace, J. M., Jones, P. D. & Kennedy, J. J. Identifying signatures of

370   natural climate variability in time series of global-mean surface temperature: Methodology

371   and insights. Journal of Climate 22, 6120–6141 (2009).

372   15. Rayner, N. et al. Improved analyses of changes and uncertainties in sea surface tempera-

373   ture measured in situ since the mid-nineteenth century: the HadSST2 dataset. Journal of

374   Climate 19, 446–469 (2006).

375   16. Thompson, D. W., Kennedy, J. J., Wallace, J. M. & Jones, P. D. A large discontinuity in

376   the mid-twentieth century in observed global-mean surface temperature. Nature 453, 646–

377   649 (2008).

378   17. Kennedy, J., Rayner, N., Smith, R., Parker, D. & Saunby, M. Reassessing biases and other

379   uncertainties in sea surface temperature observations measured in situ since 1850: 2. biases

380   and homogenization. Journal of Geophysical Research: Atmospheres 116 (2011).

381   18. Cowtan, K., Rohde, R. & Hausfather, Z. Evaluating biases in sea surface temperature

382   records using coastal weather stations. Quarterly Journal of the Royal Meteorological

383   Society 144, 670–681 (2018).

384   19. Pfeiffer, M. et al. Indian ocean corals reveal crucial role of World War II bias for Twentieth

385   Century warming estimates. Scientific Reports 7, 1–11 (2017).

386   20. Folland, C., Parker, D. & Kates, F. Worldwide marine temperature fluctuations 1856–1981.
387   Nature 310, 670–673 (1984).

388   21. Folland, C. & Parker, D. Correction of instrumental biases in historical sea surface temper-
389   ature data. Quarterly Journal of the Royal Meteorological Society 121, 319–367 (1995).

390   22. Freeman, E. et al. ICOADS Release 3.0: a major update to the historical marine climate
391   record. International Journal of Climatology 37, 2211–2232 (2017).

392   23. Kent, E. C. et al. Global analysis of night marine air temperature and its uncertainty since
393   1880: The HadNMAT2 data set. Journal of Geophysical Research: Atmospheres 118,
394   1281–1298 (2013).

395   24. Kent, E. C. et al. A call for new approaches to quantifying biases in observations of sea
396   sur- face temperature. Bulletin of the American Meteorological Society 98, 1601–1616
397   (2017).

398   25. Chan, D. & Huybers, P. Systematic differences in bucket sea surface temperature measure-
399   ments among nations identified using a linear-mixed-effect method. Journal of Climate 32,
400   2569–2589 (2019).

401   26. Chan, D., Kent, E. C., Berry, D. I. & Huybers, P. Correcting datasets leads to more homo-
402   geneous early-twentieth-century sea surface warming. Nature 571, 393 (2019).

403   27. Carella, G. et al. Estimating sea surface temperature measurement methods using charac-
404   teristic differences in the diurnal cycle. Geophysical Research Letters 45, 363–371 (2018).

28. Chan, D. & Huybers, P. Systematic differences in bucket sea surface temperatures caused by misclassification of engine room intake measurements. Journal of Climate (2020).

29. Laepple, T. & Huybers, P. Global and regional variability in marine surface temperatures. Geophysical Research Letters 41, 2528–2534 (2014).

30. Karl, T. R. et al. Possible artifacts of data biases in the recent global surface warming hiatus. Science 348, 1469–1472 (2015).

31. Davis, L. L., Thompson, D. W., Kennedy, J. J. & Kent, E. C. The importance of unresolved biases in twentieth-century sea surface temperature observations. Bulletin of the American Meteorological Society 100, 621–629 (2019).

32. Kent, E. C. et al. Observing requirements for long-term climate records at the ocean surface. Frontiers in Marine Science 6, 441 (2019).

33. Kennedy, J., Smith, R. & Rayner, N. Using AATSR data to assess the quality of in situ sea-surface temperature observations for climate studies. Remote Sensing of Environment 116, 79–92 (2012).

34. Kennedy, J., Rayner, N., Smith, R., Parker, D. & Saunby, M. Reassessing biases and other uncertainties in sea surface temperature observations measured in situ since 1850: 1. measurement and sampling uncertainties. Journal of Geophysical Research: Atmospheres 116 (2011).

35. Carella, G., Kent, E. C. & Berry, D. I. A probabilistic approach to ship voyage reconstruction in ICOADS. International Journal of Climatology 37, 2233–2247 (2017).

36. York, D., Evensen, N. M., Martınez, M. L. & De Basabe Delgado, J. Unified equations for the slope, intercept, and standard errors of the best straight line. American Journal of Physics 72, 367–375 (2004).
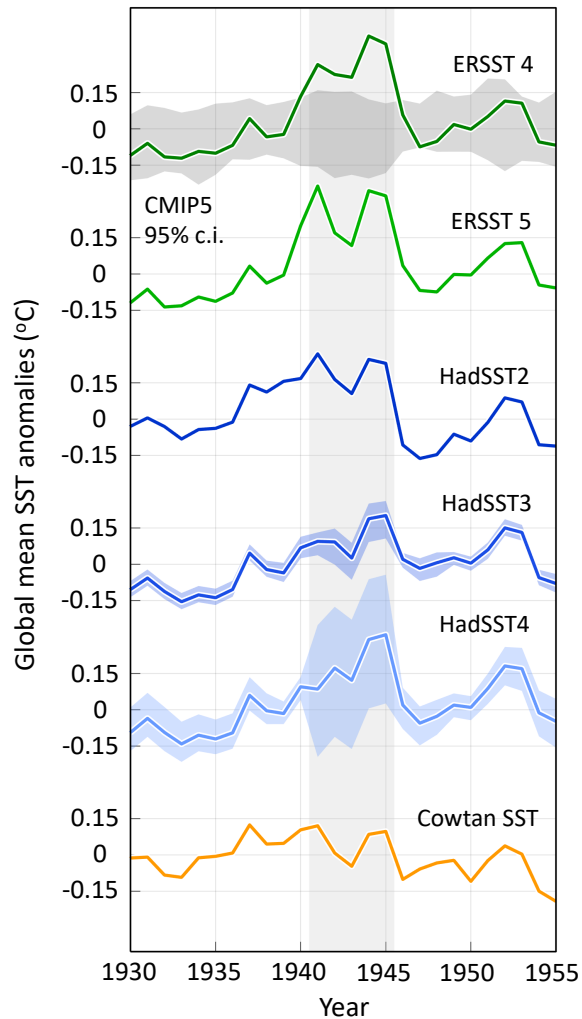
37. Woodruff, S. D. et al. Icoads release 2.5: extensions and enhancements to the surface marine meteorological archive. International journal of climatology 31, 951–967 (2011).

Acknowledgments

437 **Figures and Tables**

438

439 **Fig. 1. Various World War 2 Warm Anomalies (WW2WAs).** ERSST4 (dark green), ERSST5

440 (light green), and HadSST4 (light blue) have SSTs during WW2 that greatly exceed

441 (*P*<0.01) CMIP5 historical simulations (gray shading). HadSST3 (medium blue) and

442 Cowtan SST (orange) do not show an apparent WW2WA. Global-mean SST anomalies

443 are plotted relative to the average over 1936 to1940 and 1946 to1950 and error bars are

444 95% confidence intervals.
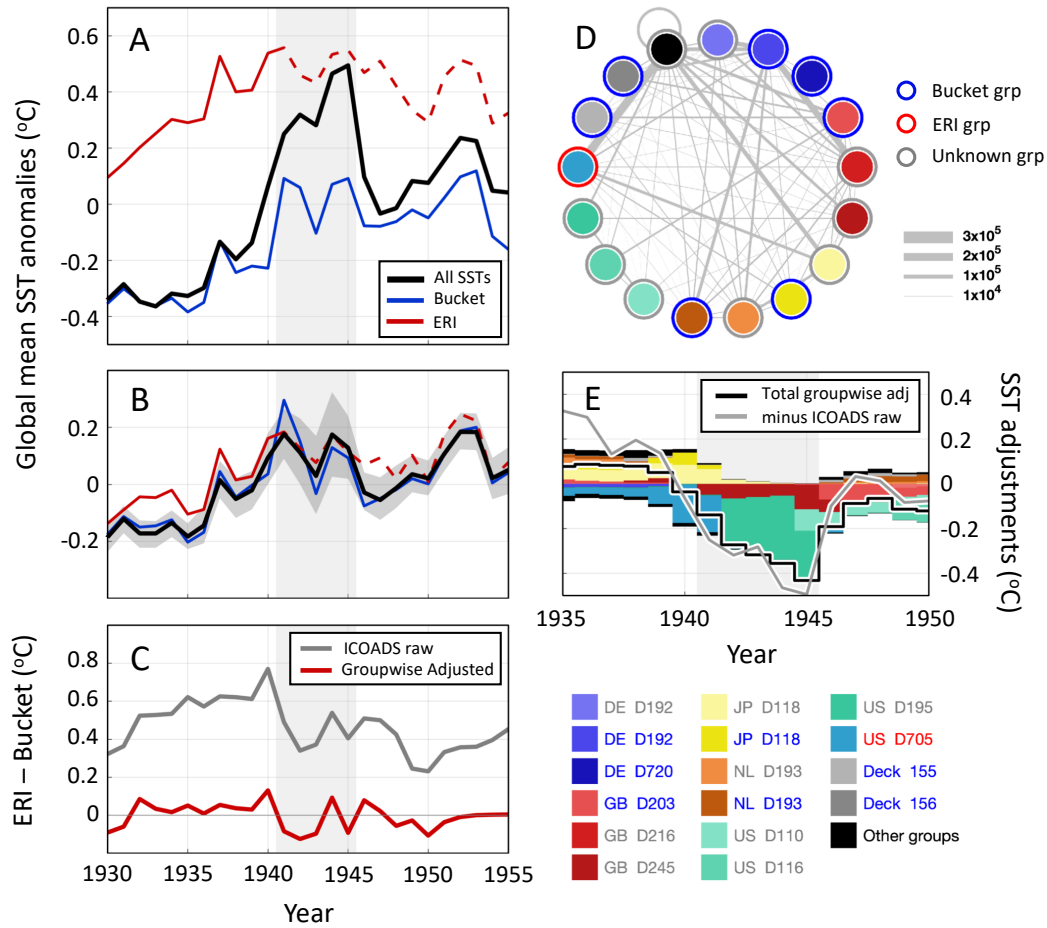
Fig. 2. Linear-mixed-effect method and groupwise SST corrections. (**A**), global mean SST anomalies in raw ICOADS dataset version 3.0. Engine-room-intake SSTs (ERI, red) are warmer than bucket SSTs (blue) throughout 1930 to 1955. Combining all available measurements (black) results in a 0.41°C WW2WA that greatly exceeds that in either bucket- or ERI-only estimates. U.S. measurements without instrumental information (dashed red) appear consistent with ERI SSTs because they have warm offsets and small-amplitude diurnal cycles (Fig. 3). (**B**), as (**A**) but after accounting for groupwise offsets, the WW2WA reduces to 0.14°C (95% c.i. 0.02 to 0.27°C, gray shading). (**C**), the difference between collocated ERI minus bucket SSTs drops from approximately 0.5°C in

455   raw ICOADS (gray) to being centered on zero after groupwise adjustments (red). (**D**),

456   numbers of SST pairs (width of connections) between individual groups (filled circles)

457   during 1935 to 1949. Groups are designated according to nation and deck number (inner

458   circle color) as well as instrument type (outer circle color). (**E**), groupwise decomposition

459   of SST adjustments (stacked bars). Adjustments during WW2 foremost relate to U.S. Navy

460   ship logs (deck 195) and G.B. Royal Navy ship's logs (deck 245). Nation abbreviations

461   are: DE, Germany; GB, Great Britain; JP, Japan; NL, the Netherlands; and US, the United

462   States. Groups having fewer than 100,000 measurements during 1935 to 1949 are labeled

463   as 'other groups'.

464
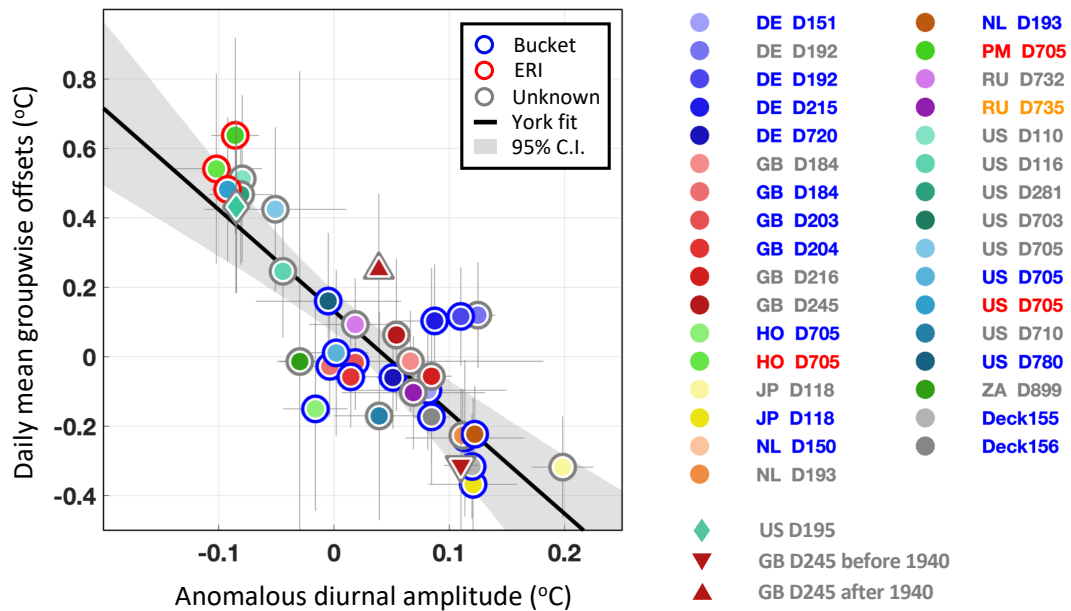
Fig. 3. Groupwise offsets scale negatively with amplitudes of diurnal cycles. Shown offsets (y-axis) are fixed and five-yearly offsets averaged over 1935 to 1949. Shown amplitudes (x-axis) are anomalies relative to the 1990 to 2014 climatology from drifters. U.S. deck 195 (diamond) mainly samples at three local hours and has its diurnal amplitude estimated using a different method (see Fig. S2). Although Great Britain deck 245 always has diurnal amplitudes significantly (*P*<0.05) higher than that from drifters, SSTs before the war (1935 to 1939, upward-pointing triangle) are coldly offset by -0.31°C, whereas SSTs after the beginning of the war (1941 to 1947, downward-pointing triangle) are warmer and have an offset 0.25°C. Colors of outer cycles denote instruments. 95% c.i.s are estimated from the linear-mixed-effect model (vertical bars on each marker) and least-squares sinusoidal fits of amplitudes (horizontal bars). The central estimate of the scaling between diurnal amplitude and offsets (black line) is from a York regression with the 95% c.i. (gray shading) estimated by bootstrapping individual groups (*28*).

478

479
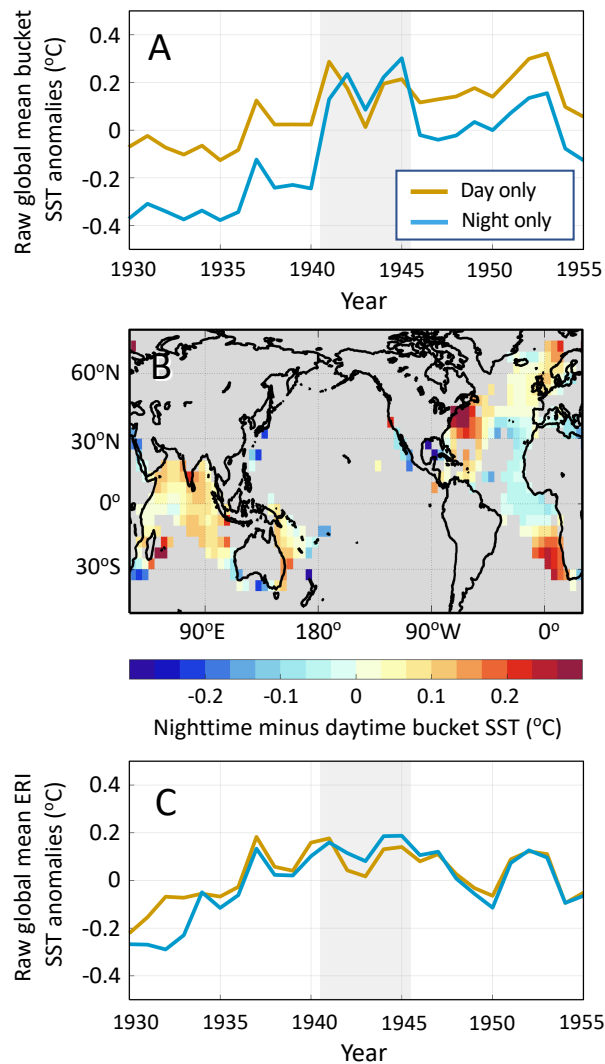
Fig. 4. Night-time bucket SSTs during WW2. (A), during WW2, night-time bucket SSTs in raw

ICOADS 3.0 data (light blue) are 0.32°C warmer than in the surrounding ten years and are

0.02°C warmer than daytime bucket SST (orange). (**B**), spatially, night-time minus

daytime bucket SSTs (shading) are positive over the Indian Ocean and the extra-tropical

Atlantic during WW2 (1942 to 1945). Grid boxes having less than three months of data

are displayed in gray. (**C**), as (**A**) but for ERI SSTs, which show no apparent WW2WA.
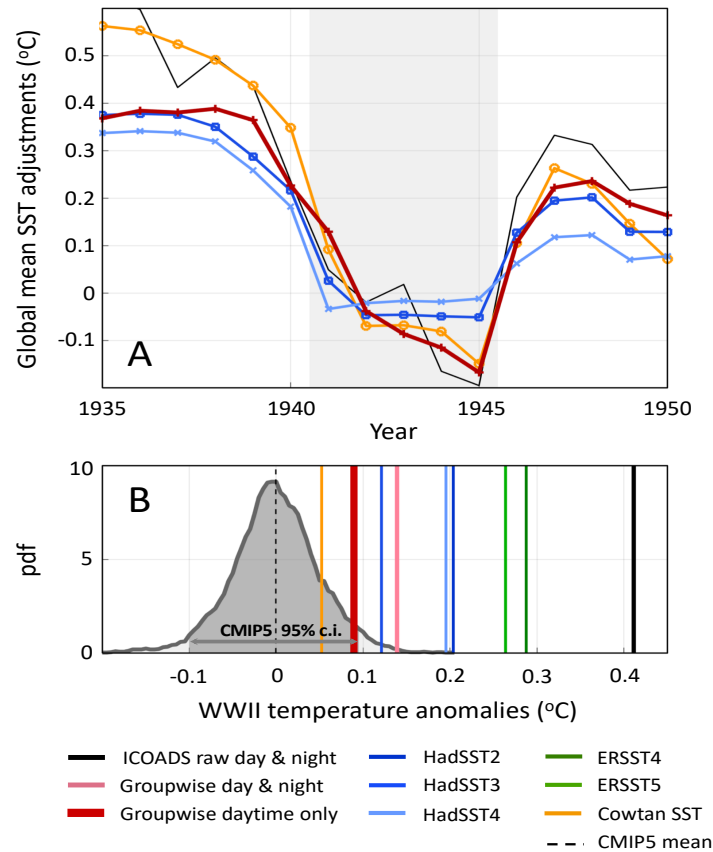
Fig. 5. Comparison against other SST estimates and model simulations. (A), SST anomalies from ICOADS 3.0 (black, reversed for purposes of comparison) along with global-mean SST adjustments from this study (red), HadSST3 (dark blue), HadSST4 (light blue), and Cowtan SST (orange). Global mean adjustments from this study are calculated as daytime groupwise- adjusted SSTs minus all unadjusted SSTs and are shifted positively by 0.22°C for purpose of comparison. (B), WW2WAs (vertical lines) are calculated as the mean difference between the average over 1941 to 1945 and the average over the ten surrounding years (1936 to 1940 and 1946 to 1950). Estimates from this study (dark red) and Cowtan (*18*) are within the 95% c.i. of internal variability (gray distribution) estimated from CMIP5 pre-industrial control simulations.

Table 1. WW2 SST anomalies and variance. The WW2WA is defined as the average over 1941--1945 minus the average over 1936 --1940 and 1946 --1950. Global-mean variance is computed from annual averages from 1936 to 1950, and regional variance is the spatial-average of interannual variance across 5°×5° grids. ERSSTs have lower regional variance because their mapping technique truncates small-scale variability. Cowtan SSTs are only available as global averages. CMIP5 models do not contain sampling and random observational errors and also show lower regional variability. Sampling and random errors cancel under averaging and become negligible at global and decadal scales (*26,34*). 95% confidence intervals are given in brackets and are estimated from available materials: 1,000 random correction members for groupwise-adjusted SSTs, 100 correction members for HadSST3, 200 correction members for HadSST4, 94 simulation members for CMIP5 historical runs, and 1,662 15-year segments for CMIP5 pre-industrial control runs.

|	WW2 Anomaly (°C)	Global-mean var. ($\times 10^{-2}$°C^2)	Average regional var. (°C^2)
ICOADS (all)	0.41	5.6	0.28
Adjusted (all)	0.14 [0.02, 0.27]	0.8 [0.4, 2.2]	0.22 [0.22, 0.23]
ICOADS (day only)	0.35	4.1	0.26
Adjusted (day only)	0.09 [-0.01, 0.18]	0.5 [0.4, 1.2]	0.21 [0.22, 0.23]
ERSST4	0.29	2.4	0.16
ERSST5	0.26	2.4	0.17
HadSST2	0.20	2.4	0.24
HadSST3	0.12 [0.03, 0.18]	0.7 [0.4, 1.1]	0.21 [0.21, 0.22]
HadSST4	0.20 [-0.09, 0.45]	1.4 [0.5, 5.3]	0.22 [0.21, 0.25]
Cowtan SST	0.05	0.6	- -
CMIP5 historical	-0.02 [-0.13, 0.07]	0.5 [0.1, 1.2]	0.13 [0.07, 0.22]
CMIP5 control	0.00 [-0.10, 0.10]	0.4 [0.1, 1.1]	0.13 [0.07, 0.20]

511   **Supplementary Materials**
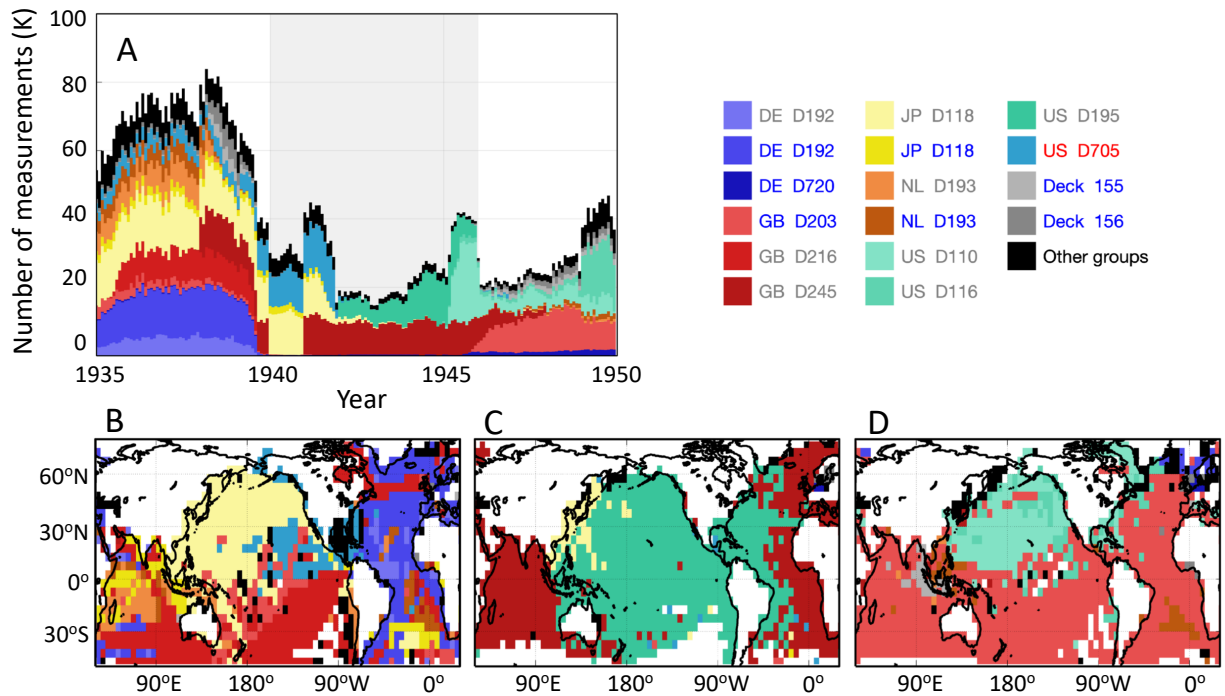
512

513   **Fig. S1. Groups of SST measurements.** (**A**) number of SST measurements from individual

514   groups identified by country, deck, and instrument.   Nation abbreviations are: DE,

515   Germany; GB, Great Britain; JP, Japan; NL, the Netherlands; and US, the United States.

516   Groups having fewer than 100,000 measurements between 1935 and 1949 are labeled as

517   'other groups'.   Instruments are indicated by the color of group names for bucket (blue),

518   ERI (red), and unknown method (gray). (**B-D**), maps indicating groups that contribute the

519   most observations within 5° grid boxes for 1936 to 1940 (**B**), 1941 to 1945 (**C**), and 1946

520   to 1950 (**D**).   White grid boxes have fewer than three years of data within corresponding

521   5-year   intervals.

522

523
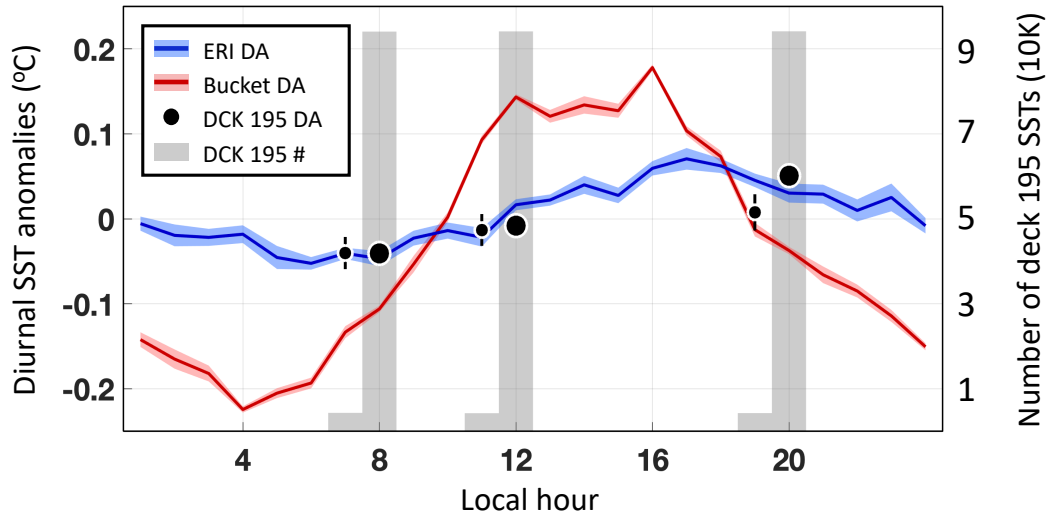
Fig. S2. The diurnal amplitude of U.S. deck 195. 96% measurements of SSTs from U.S. deck 195 are sampled at 8 am, 12 pm, and 8 pm (gray bars, right y-axis), which does not meet the required minimum number of measurements in each 6-hourly bin in a day for estimating diurnal amplitudes using a sinusoidal fit (*27, 28*). We, therefore, take an alternative approach that uses diurnal cycles from bucket (red) and ERI (blue) measurements as templates. Diurnal anomalies of bucket and ERI SSTs are obtained from tracked ships over 1935 to 1949 and are shifted such that the mean over 8 am, 12 pm, and 8 pm is zero. Unknown U.S. measurements from decks other than 195 are assumed to be ERI measurements. Specifically, diurnal anomalies of deck 195 are represented as a linear combination of bucket and ERI cycles, with the mixture determined using least-squares fitting. The best fit yields 115% ERI and -15% bucket, equivalent to a diurnal amplitude of 0.04°C that is 0.08°C smaller than that of drifting buoys. A percentage higher than 100% should be interpreted as a smaller amplitude than other ERI groups, possibly associated with a deeper sampling depth of large naval ships.

538

539
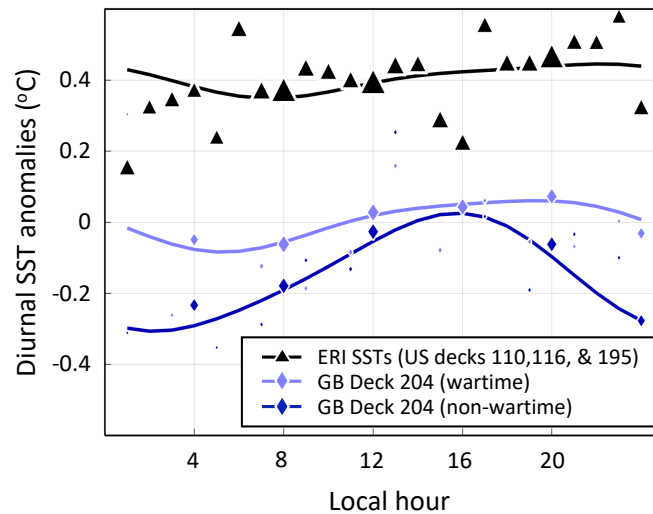
Fig. S3. Warm biases in night-time bucket SSTs during WW2. Night-time SSTs from British deck 204 are anomalously warmer during the war (1941 to 1945, light blue) than surrounding years (dark blue). To obtain diurnal anomalies in this figure, we bin all measurements by local hour and calculate the mean in each bin. Such a method is less rigorous than that uses tracked ships (*28*) but allows for using the maximum amount of data and for a qualitative investigation of offsets between periods. To control noise arising from sampling different regions, we remove collocated groupwise-adjusted daytime SSTs on monthly 5° grids before binning. Results are first calculated for individual years and then averaged over respective periods. Smoothed diurnal cycles are determined with once- and twice-per-day sinusoidal harmonics using a least-square fitting weighted by numbers of measurements in each hourly bin. Also shown are diurnal anomalies of ERI SSTs estimated from U.S. decks 110, 116, and 195. Other U.S. decks are excluded because they take SSTs at fixed Greenwich rather than local hours, which induces additional noise by preferentially sampling certain regions at different local hours.

554
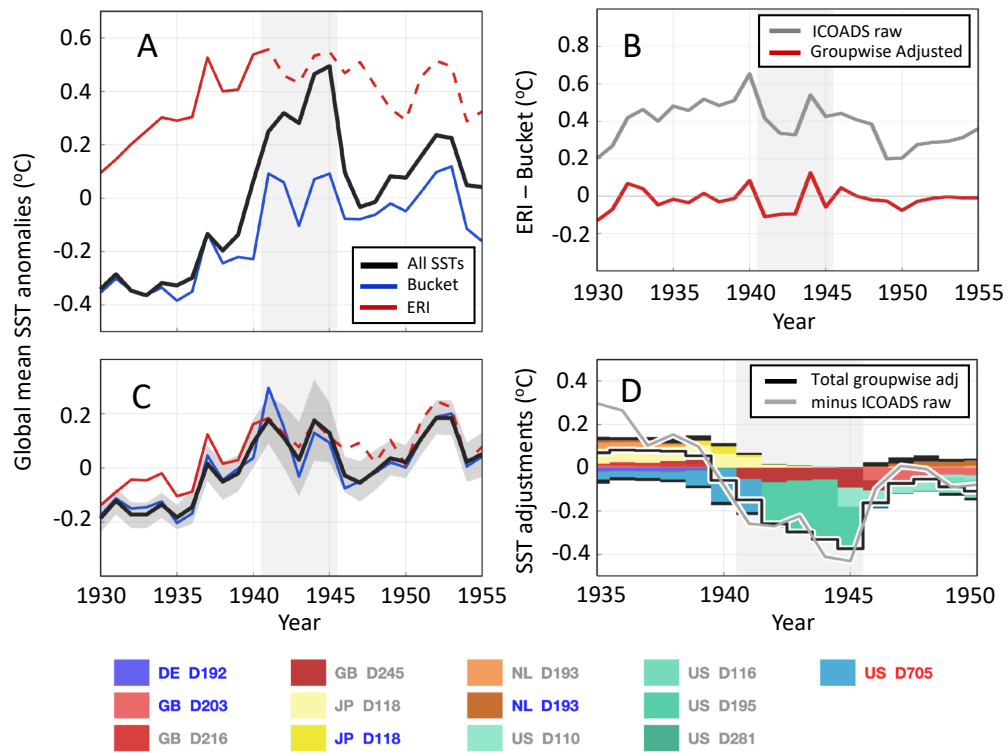
Fig. S4. Groupwise corrections for daytime SSTs. Individual panels are as those in Fig. 2 but

for the LME analysis that only uses daytime measurements.
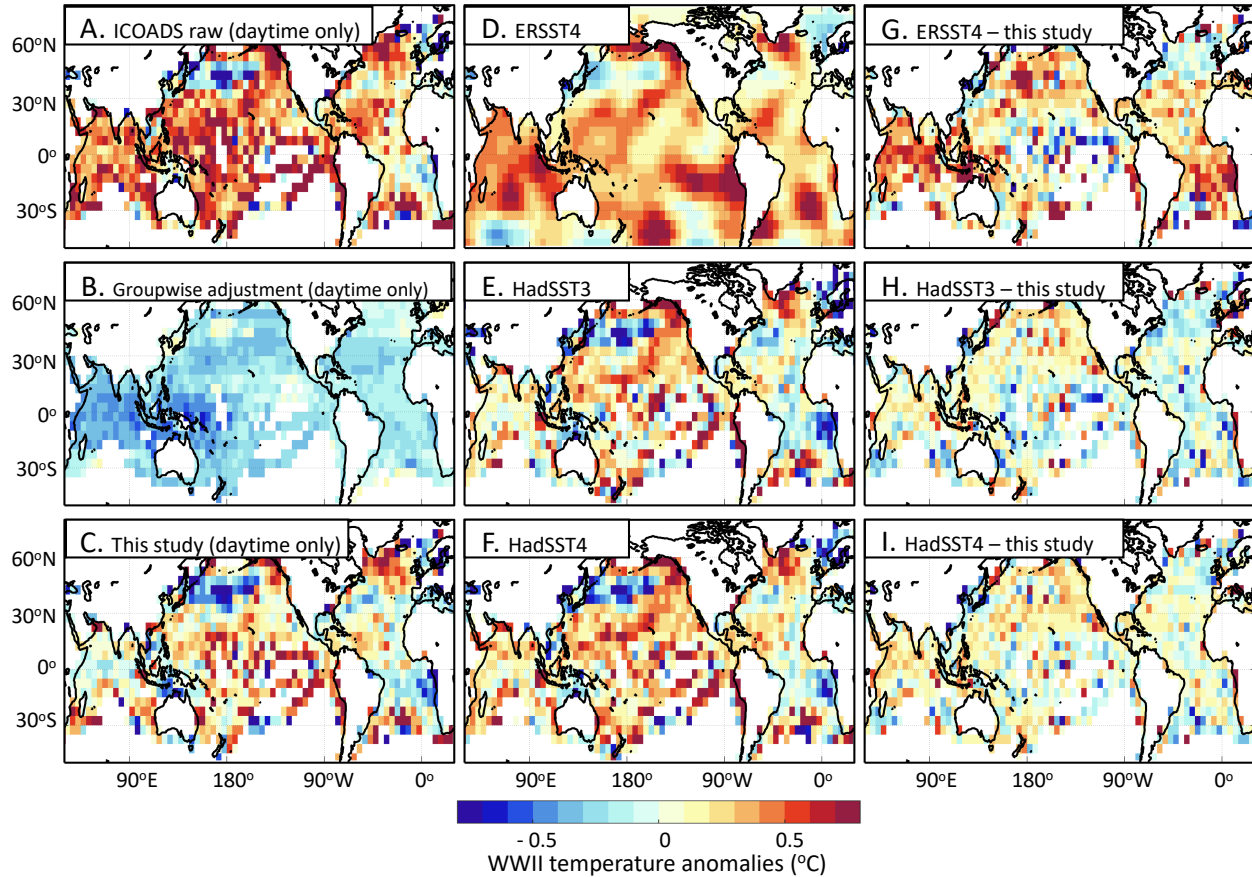
Fig. S5. Patterns of WW2 SST anomalies. Shown temperature difference are between 1941 to 1945 and the mean over 1936 to 1940 and 1946 to 1950 for (**A**), raw daytime SSTs in ICOADS 3.0, (**B**), groupwise adjustments of daytime SSTs, (**C**), adjusted daytime SSTs (**A** plus **B**), (**D**), ERSST4 (ERSST5 has a similar pattern), (**E**), HadSST3, and (**F**), HadSST4. A grid box is shown if it has at least one year of data that each has at least six months (a valid year) of observations during 1941 to 1945 and at least one valid year of data during the ten surrounding years. Also shown are comparisons of our adjusted WW2WA with other estimates from (**G**), ERSST4, (**H**), HadSST3, and (**I**), HadSST4.

568 **Table S1. Groups containing SST measurements during 1935 to 1949.** Among 66 groups

569 that have groupwise offset estimates, 33 have valid estimates for the amplitude of diurnal cycles.

570 Shown LME offsets are mean offsets averaged over 1935 to 1949 for the analysis that uses both

571 daytime and night-time SSTs and the analysis that only uses daytime SSTs, respectively. Diurnal

572 amplitudes are anomalies relative to collocated climatology estimated from drifting buoys. '*'

573 indicates groupwise offsets differing from zero (*P*<0.05) or diurnal amplitudes differing that of

574 drifting buoys (*P*<0.05). '**' indicates significance after Bonferroni corrections (*P*<0.05/66 for

575 groupwise offsets and *P*<0.05/33 for diurnal amplitudes). Checkmarks highlight U.S. groups with

576 unknown methods, which are assumed to contain ERI SSTs when computing ERI-only estimates.

Group	Nation	Deck	Method - ICOADS SI	# of Meas.	Mean offsets	Day offsets	Excess DA	
DE DCK 151	German	Pacific HSST German Receipts	Bucket	3K	-0.10	-0.07	0.08*	
DE DCK 192	German	Deutsche Seewarte Marine	Unknown	259K	0.12	0.13	0.13**	
DE DCK 192	German	Deutsche Seewarte Marine	Bucket	707K	0.12	0.10	0.11**	
DE DCK 215	German	German Marine	Bucket	35K	0.10	0.13	0.09**	
DE DCK 720	German	Deutscher Wetterdienst Marine Met. Archive	Bucket	103K	-0.06	-0.12	0.05**	
GB DCK 184	Great Britain	Great Britain Marine	Unknown	10K	-0.01	-0.02	0.07	
GB DCK 184	Great Britain	Great Britain Marine	Bucket	62K	-0.03	-0.02	-0.00	
GB DCK 203	Great Britain	Selected UK Ships	Bucket	568K	-0.02	0.01	0.02**	
GB DCK 204	Great Britain	British Navy (HM) Ships	Bucket	71K	-0.06	-0.09	0.01	
GB DCK 216	Great Britain	UK Merchant Ship logbooks	Unknown	415K	-0.06	-0.07	0.08**	
GB DCK 245	Great Britain	Royal Navy Ship's Logs	Unknown	901K	0.06	0.04	0.05**	
HO DCK 705	- -	US Merchant Marine Collection (series 500)	Bucket	13K	-0.15	-0.17	-0.02	
HO DCK 705	- -	US Merchant Marine Collection (series 500)	ERI	21K	0.54**	0.47**	-0.10**	
JP DCK 118	Japan	Kobe Collection data	Unknown	1056K	-0.32**	-0.28**	0.20**	
JP DCK 118	Japan	Kobe Collection data	Bucket	178K	-0.37*	-0.31*	0.12**	
NL DCK 150	Netherlands	Pacific HSST Netherlands Receipts	Bucket	9K	-0.23*	-0.23	0.11**	
NL DCK 193	Netherlands	Netherlands Marine	Unknown	296K	-0.23*	-0.17*	0.11**	
NL DCK 193	Netherlands	Netherlands Marine	Bucket	227K	-0.22*	-0.20*	0.12**	
PM DCK 705	- -	US Merchant Marine Collection (series 500)	ERI	27K	0.64**	0.55**	-0.09**	
RU DCK 732	Russia	Russian Marine Met Data Set	Unknown	52K	0.09	0.02	0.02	
RU DCK 735	Russia	Russian Research Vessel	Hull sensor	1K	-0.10	-0.11	0.07*	
US DCK 110	United States	US Navy Marine	Unknown	402K	0.51**	0.45**	-0.08**	√
US DCK 116	United States	US Merchant Marine	Unknown	234K	0.25*	0.19*	-0.04**	√
US DCK 281	United States	US Navy Monthly Aerological Record	Unknown	90K	0.47**	0.41**	-0.08**	√
US DCK 703	United States	US Lightship Collections	Unknown	17K	-1.08**	-1.02**	0.03	√
US DCK 705	United States	US Merchant Marine Collection (series 500)	Unknown	26K	0.42**	0.39**	-0.05	√
US DCK 705	United States	US Merchant Marine Collection (series 500)	Bucket	99K	0.01	-0.03	0.00	√
US DCK 705	United States	US Merchant Marine Collection (series 500)	ERI	542K	0.48**	0.45**	-0.09**	

US DCK 710	United States	US Arctic Logbooks	Unknown	2K	-0.17	0.02	0.04*	√
US DCK 780	United States	NOAA World Ocean Database	Bucket	9K	0.16	0.11	-0.00	
ZA DCK 899	South Africa	South Africa Whaling	Unknown	13K	-0.01	-0.12	-0.03**	
DCK 155	- -	Indian HSST	Bucket	119K	-0.32**	-0.23	0.12**	
DCK 156	- -	Atlantic HSST	Bucket	189K	-0.17*	-0.15*	0.08**	
BX DCK 706	- -	US Merchant Marine Collection (series 600)	Unknown	5K	-0.10	-0.15	- -	
CN DCK 706	China	US Merchant Marine Collection (series 600)	Unknown	1K	-0.38*	-0.43**	- -	
DL DCK 706	- -	US Merchant Marine Collection (series 600)	Unknown	2K	0.07	0.04	- -	
DN DCK 706	- -	US Merchant Marine Collection (series 600)	Unknown	3K	-0.12	-0.04	- -	
FR DCK 706	France	US Merchant Marine Collection (series 600)	Unknown	7K	0.42**	0.39**	- -	
GB DCK 152	Great Britain	Pacific HSST UK Receipts	Bucket	<1K	-0.04	-0.05	- -	
GB DCK 202	Great Britain	All Ships (UK MetO MDB)	Bucket	<1K	-0.06	-0.03	- -	
GB DCK 205	Great Britain	Scottish Fishery Cruisers	Bucket	4K	-0.43*	-0.39*	- -	
GB DCK 705	Great Britain	US Merchant Marine Collection (series 500)	Bucket	18K	-0.12	-0.07	- -	
GB DCK 705	Great Britain	US Merchant Marine Collection (series 500)	ERI	11K	0.13	0.08	- -	
GB DCK 706	Great Britain	US Merchant Marine Collection (series 600)	Unknown	23K	-0.03	-0.09	- -	
GB DCK 707	Great Britain	US Merchant Marine Collection (series 700)	Unknown	<1K	-0.19	-0.26*	- -	
HO DCK 706	Great Britain	US Merchant Marine Collection (series 600)	Unknown	<1K	0.05	0.00	- -	
HO DCK 707	Great Britain	US Merchant Marine Collection (series 700)	Unknown	<1K	0.09	0.05	- -	
IY DCK 706	Great Britain	US Merchant Marine Collection (series 600)	Unknown	6K	0.19	0.20*	- -	
JP DCK 705	Japan	US Merchant Marine Collection (series 500)	Unknown	10K	-0.31*	-0.27*	- -	
JP DCK 705	Japan	US Merchant Marine Collection (series 500)	Bucket	26K	-0.38*	-0.35*	- -	
JP DCK 705	Japan	US Merchant Marine Collection (series 500)	ERI	5K	-0.31*	-0.31*	- -	
JP DCK 706	Japan	US Merchant Marine Collection (series 600)	Unknown	8K	-0.26*	-0.28**	- -	
NL DCK 705	Netherlands	US Merchant Marine Collection (series 500)	Bucket	10K	-0.21	-0.19	- -	
NL DCK 706	Netherlands	US Merchant Marine Collection (series 600)	Unknown	17K	-0.18	-0.14*	- -	
NO DCK 706	Norway	US Merchant Marine Collection (series 600)	Unknown	3K	0.34*	0.31**	- -	
PM DCK 707	- -	US Merchant Marine Collection (series 700)	Unknown	<1K	0.59**	0.46*	- -	
RU DCK 735	Russia	Russian Research Vessel	Bucket	<1K	-0.05	- -	- -	
SP DCK 706	- -	US merchant Marine Collection (series 600)	Unknown	<1K	0.01	-0.01	- -	
US DCK 116	United States	US Merchant Marine	Bucket	13K	-0.12	-0.14	- -	
US DCK 195	United States	US Navy Ships Logs	Unknown	383K	0.43**	0.39**	- -	√
US DCK 706	United States	US Merchant Marine Collection (series 600)	Unknown	51K	0.28*	0.29**	- -	√
US DCK 707	United States	US Merchant Marine Collection (series 700)	Unknown	2K	0.30*	0.27*	- -	√
US DCK 780	United States	NOAA World Ocean Database	Unknown	1K	0.22*	0.20*	- -	√
ZA DCK 927	South Africa	International Marine	Unknown	17K	0.01	0.01	- -	
DCK 197	- -	Danish (and other) Marine (Polar)	Unknown	3K	-0.12	-0.06	- -	
DCK 255	- -	Undocumented TDF-11 Decks or MDB Series	Bucket	<1K	0.10	0.13	- -	

577

578